

南華大學科技學院永續綠色科技碩士學位學程

碩士論文

Master Program of Green Technology for Sustainability

College of Science and Technology

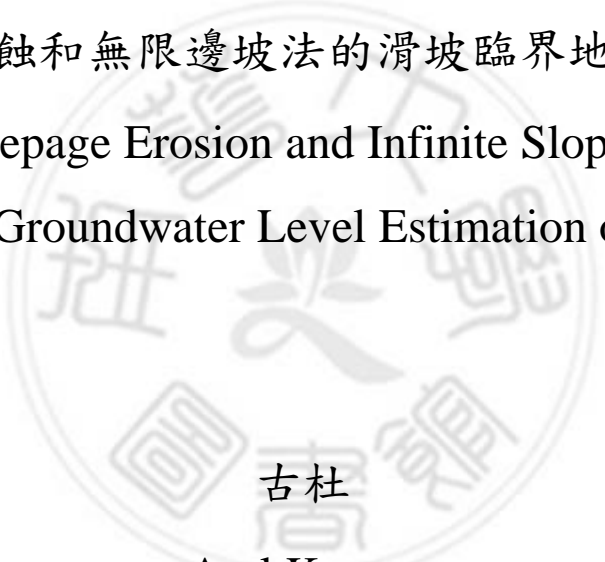
Nanhua University

Master Thesis

基於滲流侵蝕和無限邊坡法的滑坡臨界地下水位估算

Using the Seepage Erosion and Infinite Slope Method on

the Critical Groundwater Level Estimation of Landslide



古杜

Atul Kumar

指導教授：洪耀明 博士

Advisor: Yao-Ming Hong, Ph.D.

中華民國 109 年 6 月

June 2020

# 南華大學

科技學院永續綠色科技碩士學位學程

碩士學位論文

基於滲流侵蝕和無限邊坡法的滑坡臨界地下水位估算

Using the Seepage Erosion and Infinite Slope Method on the Critical  
Groundwater Level Estimation of Landslide

研究生： Atul kumar

經考試合格特此證明

口試委員： 朱新

吳志元

洪耀明

指導教授： 洪耀明

系主任(所長)： 洪耀明

口試日期：中華民國 109 年 6 月 29 日

## ACKNOWLEDGEMENT

First of all I would like to thank my thesis advisor professor Hong Yao Ming president of green technology for sustainability from Nanhua University. I would like to express my special thanks of gratitude to my teacher Chen Bo-Ching, it is because of their guidance helped me in all the time of research and writing of this thesis. Professor Hong Yao Ming was always there for me whenever needed weather i have any question or any kind of trouble. He give me new ideas and always allowed me to think out of the box and guided me how to turn ideas into reality. I would like to thank all my loved ones, who have supported me throughout this entire process, by helping me putting pieces together. I will be grateful forever for your love. Thanks to my classmate and friends for always being there for me whenever needed in my good and bad times or when I get trouble in lab about equipment, no matter what the problem was they were always ready to help and support in my research field. Last but not the least I would like to thank God and my family, for supporting me spiritually throughout writing this thesis and my life in general. I wish to thank all the people whose assistance was a milestone in the completion of this project. This accomplishment would not have been possible without them.

Thank you.

Atul kumar

Department of Green Technology for Sustainability

Nanhua University, Taiwan, R.O.C.

## 中文摘要

地下水滲漏往往導致災難性的邊坡破壞。河岸、運河和水庫堤壩和山坡象徵著觀察到滲漏侵蝕的情況。在土壤侵蝕研究和與穀物顆粒運輸相關的研究中，細顆粒的分離和動員是重要的考慮因素。通過孔隙水流動引起的物理和化學效應可以分離細黏土顆粒。化學作用包括通過增加顆粒、顆粒排斥力將黏土顆粒黏合到砂粒上的黏合劑溶解和顆粒分散。本文描述了地下水位的上升將降低土壤濃度，增加相互平行的滲流侵蝕和滑坡的破壞。在本文中，使用理論研究探討臨界剪切應力( $\tau_c$  值)和內聚力(C)之間的關係。該研究還考慮了地表附近風化和孔隙度對土壤摩擦角變化的影響。安全係數被概念化為深度的函數。在沙質和粉質土壤上進行邊坡穩定性分析。研究了土壤樣品特徵的深入研究，並計算了一些重要數據和信息，如從監測壓實實驗中獲得的最大干密度，使用篩分分析度分佈，使用常數求得的滲透率常數值(K 值)頭和落頭的方法。這些分析表明，對於沙質和粉質土壤的坡面，在穩定入滲條件下，地下水位以上都會發生破壞，這與經典無限斜率理論無法預測的一些野外觀測結果一致。

關鍵詞: 無限斜率、滲流、臨界地下水位、臨界流線長度、內聚力

## ABSTRACT

This paper has tried to establish relationship between rainfall and groundwater level, and calculate the critical height of groundwater level that triggers landslide. Groundwater seepage has often leads to catastrophic slope failure. River bank, canal and reservoir embankment and hill slope symbolizes situation where seepage erosion has been observed. The present paper describes the rising of groundwater level will reduce the soil concentration and raise the damage of seepage erosion and landslide which occur parallel to each other. In this paper, the relationship between critical shear stress ( $\tau_c$  value) and cohesion (C) is explored using theoretical investigations. The study also considers the effect of weathering and porosity near the ground surface on changes in the friction angle of the soil. The factor of safety is conceptualized as a function of depth. Slope stability analysis is done on sandy and silty soil. A deep study on the characteristic of soil sample is studied along with calculating some important data and information like, the maximum dry density obtained from the proctor compaction experiment, particles size distribution classified using sieve analysis, permeability constant values (K values) found using constant head and falling head method. These analyses indicate that for hill-slopes of both sandy and silty soils, failure can occur above the water table under steady infiltration conditions, which is consistent with some field observations that cannot be predicted by the classical infinite slope theory.

**Keywords:** Infinite slope, Seepage, Critical groundwater level, Critical streamline length, Cohesion

# TABLE OF CONTENT

ACKNOWLEDGEMENT .....	I
中文摘要.....	II
ABSTRACT.....	III
TABLE OF CONTENT.....	IV
LIST OF FIGURES .....	VI
LIST OF TABLE .....	VIII
Chapter-1 Preface .....	1
1.1 Introduction.....	1
1.2 Purpose.....	2
Chapter-2 Literature Review .....	3
2.1 Soil Consistency.....	4
2.2 Seepage analysis.....	6
2.3 Ball test.....	7
Chapter-3 Theory.....	11
3.1 Prediction methodologies.....	11
3.2 Judgmental approach which is based on landslide typology.....	11
3.3 Infinite slope theory.....	13
3.4 The infinite slope method.....	15
3.5 Darcy law equation.....	17
3.6 The Mohr coulomb failure criteria.....	18
Chapter-4 Outcome and discusson .....	21
4.1 Standard Proctor compaction test.....	21
4.2 Falling head permeability test.....	24
4.3 Test for Threshold Pressure .....	27
4.4 Tri-axial Test.....	29

Chapter-5 Discussion.....42  
Chapter-6 Conclusion ..... 43  
References..... 44



## LIST OF FIGURES

<b>Figure 2.1</b> Ball Test.....	07
<b>Figure 3.1</b> Forces acting on the slip surface.....	14
<b>Figure 3.2</b> Infinite slope .....	15
<b>Figure 3.3</b> Mohr coulomb failure for Cohesion-less soil .....	19
<b>Figure 3.4</b> Mohr coulomb failure for Cohesive soil.....	19
<b>Figure 3.5</b> Mohr coulomb failure for cohesive frictional soil.....	19
<b>Figure 4.1</b> Mixing Tray sand.....	21
<b>Figure 4.2</b> Sample graph for compaction.....	23
<b>Figure 4.3</b> Permeability meter.....	25
<b>Figure 4.4</b> Constant head permeability test.....	25
<b>Figure 4.5</b> Configuration of permeability test.....	26
<b>Figure 4.6(a)</b> Experiment setup for NEFT test.....	27
<b>Figure 4.6(b)</b> Air pressure gauge.....	27
<b>Figure 4.6(c)</b> Pressure adjustment valve.....	27
<b>Figure 4.7</b> Layout diagram of NEFT.....	28
<b>Figure 4.8</b> Tri-axial test cell.....	29
<b>Figure 4.9(a)</b> Cell manual control.....	30



<b>Figure 4.9(b)</b> Air/water control.....	30
<b>Figure 4.9(c)</b> Tri-axial cell.....	30
<b>Figure 4.9(d)</b> Load frame.....	30
<b>Figure 4.9(e)</b> Displacement transducer.....	30
<b>Figure 4.9(f)</b> Volume controller.....	30
<b>Figure 4.10</b> Tri-axial shear test display process.....	33
<b>Figure 4.11</b> Tri-axial shear test display process.....	33
<b>Figure 4.12</b> Schematic diagram of Tri-axial shear test experiment.....	34
<b>Figure 4.13</b> Graph for Deviator stress versus axial strain curve .....	35
<b>Figure 4.14</b> Graph for volumetric strain versus axial strain curves.....	36
<b>Figure 4.15</b> Mohr's circle failure.....	37
<b>Figure 4.16</b> Graph of slope of critical ground water level.....	40

## LIST OF TABLE

<b>Table1.</b> Plastic limit and liquid limit.....	05
<b>Table2.</b> Plasticity of various silt/clay soils.....	06
<b>Table3.</b> Calculation for dry density.....	22
<b>Table4.</b> Calculation for water content.....	23
<b>Table5.</b> Falling head permeability test .....	26



## Chapter-1 Preface

### *1.1 Introduction*

In general, rainfall-induced slope failures are caused by increased pore pressure and seepage force during periods of intense rainfall. The effective stress in the soil decreases due to the increased pore pressure, reducing the soil shear strength, and ultimately resulting in slope failure. Landslide usually occurs in the condition or in the area that have high groundwater level. Ground water drainage has regularly prompts cataclysmic slant disappointment. Waterway bank, trench and store dike and slope incline represents circumstance where drainage disintegration has been watched. Terzaghi (1950), avalanche specialists have endeavoured to more readily comprehend and foresee calamitous incline disappointment. Separation and assembly of fine particles are significant contemplations both in soil disintegration examines and in considers identified with transportation of grain particles. Separation of fine mud particles is conceivable both by physical and substance impacts actuated through pore-water stream. The synthetic impacts incorporate disintegration of the establishing operators that dilemma dirt particles to sand grains and scattering of particles by expanding molecule ghastly forces. According the perception of research facility explore, the leakage erosion will deliver a funnel in the slip slant. After the funnel size arrives at a basic worth , the destabilize powers will be greater than the opposing power, and that will prompt happens avalanche .Therefore, it's the motivation behind why heap structure is typically worked in the toe of slant to forestall the leakage disintegration and the vast majority of the slant security examinations have been founded on Terzaghi's viable pressure standard wherein pore water pressure is evaluated by soaked drainage speculations.

## *1.2 Purpose*

There are many main causes of collapse, including factors such as rise of groundwater level, rock joints and underground seepage. If factors such as rock joints are ignored, infinite slope theory and seepage theory can be integrated. This study uses the theory formed by Hong (2018) through laboratory tests and experiment, which helps to calculate the critical groundwater level and streamline length of collapsed land, and calculation of critical value of seepage To obtain the parameters required by the theory, and then indirectly test to verify the correctness of the theory



## Chapter-2 Literature Review

There are basically three types of soil: sand, silt and clay. But, most of the soils are composed by the combination of the soil in different ratios. How they mix will determine the texture of the soil or in other words, how the soil looks and feels. Surface grains of sediment are acted by 3 force. (1) Tractive forces: horizontal force exerted by water. (2) Local seepage forces: it acts in vertical downward direction.(3) Gravity (universal force). The critical shear stress concept was later utilized by Khilaretal (1985) who developed a capillary model predicting the conditions necessary for clay particle detachment due to applied shear stresses. Khilaretal. (1985) postulated that internal erosion of soils is a two-step process consisting of particle detachment and particle migration. They concluded that the migration of particles was largely governed by two variables: (1) the size distribution of the migrating particles relative to the pore size distribution of the medium, and (2) the concentration of the eroded particles in the pore fluid. Similar studies were conducted by Hubbe (1985a, 1985b, 1987a, 1987b) and Sharmaetal. (1992) in an attempt to understand the hydrodynamic force required to detach particles from flat surfaces. Paper of Yao-Ming Hong, and (Terzaghi and Peck 1967;Hutchinson 1968, 1982; Hi; Iverson and Major 1986; Jones 1990; Dunne 1990; Koenders and Selimeyer 1992; Worman 1993; Skempton and Brogan 1994). However distinctions have been made by some investigators between different mechanisms involved in the instability caused by seepage (Dunne 1990; Crosta and Prisco 1999)

## *2.1 Soil Consistency.*

Soil consistency is the quality with which soil materials are held together or the opposition of soils to twisting and burst. Soil consistency is estimated for wet, soggy and dry soil tests. For wet soils, it is communicated as both tenacity and versatility. Assurance of dry-soil consistency utilizing the Atterberg Limits Testing is done when the dirt has been air-dried.

Attempt to break a modest quantity of dry soil by squeezing it between your thumb and index finger or by crushing it in the palm of your hand.

- 1) Loose, if the dirt is non-reasonable (single-grain structure).
- 2) Soft, if the dirt is feebly sound and friable. breaking to powder or individual grains under extremely slight tension.
- 3) Slightly hard, if the dirt opposes light weight, yet can be broken effectively among thumb and index finger.
- 4) Hard, if the dirt opposes moderate weight, can scarcely be broken between the thumb and index finger, however can be broken in the hands without trouble.
- 5) Very hard, if the dirt opposes incredible weight, can't be broken between the thumb and pointer yet can be broken in the hands with trouble.
- 6) Extremely hard, if the dirt opposes extraordinary weight and can't be broken in the hands.

Typical laboratory tests of average LL and PL (percentages moisture)

**Table 1:** Average LL and PL

SOIL TYPE	Liquid limit (LL %)	Plastic limit(PL%)
Sand	20	0
Silt	27	20
Clay	100	45
Colloidal clays	399	46

Data reference is from Soil Mechanics and Foundations by Dr. B. C. Punmia Ashok Kumar Jain A. K. Jain(2005-12-15)

Calculation of the plasticity index and its significance: Based on as far as possible and as far as possible, the versatility record (PI) can be characterized as the numerical distinction between fluid breaking point and plastic cutoff showing below

$$PI = LL - PL$$

Fluid cutoff (LL): The rate dampness content at which a dirt changes with diminishing wetness from the fluid to the plastic consistency or with expanding wetness from the plastic to the fluid consistency.

Plastic breaking point (PL): The rate dampness content at which a dirt changes with diminishing wetness from the plastic to the semi-strong consistency or with expanding wetness from the semi-strong to the plastic consistency

**Table 2:** Display the plasticity of various silt and clay soils

Category	Soil	PI (percentage)	Degree of plasticity
I	Sand or silt • Traces of clay • Little clay	0-1	Non-plastic
		1-5	Slight plasticity
		5-10	Low plasticity
II	Clay loam	10-20	Medium plasticity
III	Silt clay Clay	20-35	High plasticity
		>35	Very high plasticity

Data reference Data reference is from Soil Mechanics and Foundations by Dr. B. C. Punmia Ashok Kumar Jain A. K. Jain (2005-12-15)

The relationship between liquid limit and plastic index can be used to classify the fine soil particle size. Plastic limit and liquid limit is extremely useful for understanding soil behavior of fine soil particles. These limits are very important soil characteristics and don't change but it remain constant for the entire life.

## 2.2 Seepage analysis

Leakage investigation Assuming that the impact of pore-pneumatic force is immaterial and that water stream because of the warm angles is thought to be unimportant. In one-dimensional uniform stream in a soaked soil can be characterized by a changed type of Richards condition (Richards, 1931). Along these lines, the stream in an unsaturated unending soil slant can be portrayed by the 1D condition reference from ( Zhan et al., 2012 ). This overseeing condition is given by Zhanetal and Richardson.



$$\frac{d\theta}{dt} = \frac{d}{dz} \left( k \left[ \frac{du}{dz} + \cos \alpha \right] \right) \quad (1)$$

where  $\theta$ , is the volumetric water content,  $t$ , is time  $u$ , is the pore water pressure head,  $\alpha$  is the inclination of the slope to the horizontal,  $K$  is the hydraulic conductivity and  $z$  is the spatial coordinate.

### 2.3 Ball test

It is method using rheology test to know about the shear stress of soil. This theory is based on Navier Stokes incompressibility theory equation of equilibrium on three dimensional body of soil solids and the concept of this experiment is based on Stokes law

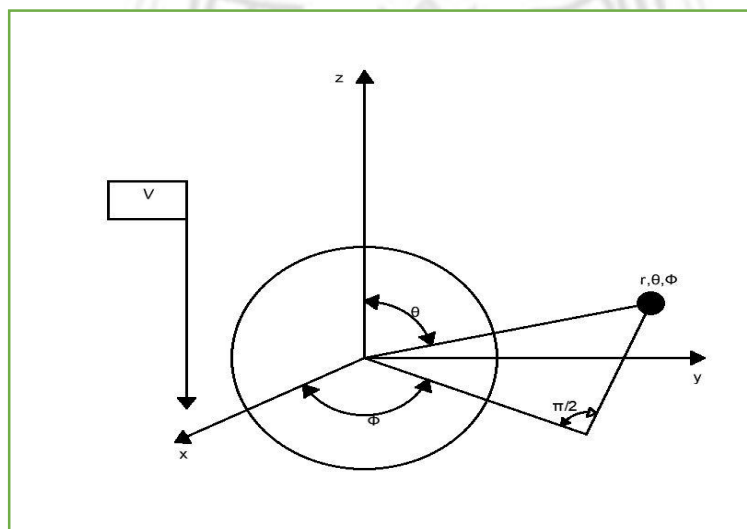


**Figure 2.1:** Reference source Stokes, G. G. (1851). "On the effect of internal friction of fluids on the motion of pendulums

$r, \theta, \phi$  = coordinates of ball in  $x, y, z$  direction in 3D space

$$\rho \frac{\partial v_x}{\partial t} = \frac{\partial p}{\partial y} + \rho g_x + \eta \left( \frac{\partial^2 v_x}{\partial x^2} + \frac{\partial^2 v_x}{\partial y^2} + \frac{\partial^2 v_x}{\partial z^2} \right) \quad (1a)$$

$$\rho \frac{\partial v_y}{\partial t} = \frac{\partial p}{\partial x} + \rho g_y + \eta \left( \frac{\partial^2 v_y}{\partial x^2} + \frac{\partial^2 v_y}{\partial y^2} + \frac{\partial^2 v_y}{\partial z^2} \right) \quad (1b)$$

$$\rho \frac{\partial v_z}{\partial t} = \frac{\partial p}{\partial z} + \rho g_z + \eta \left( \frac{\partial^2 v_z}{\partial x^2} + \frac{\partial^2 v_z}{\partial y^2} + \frac{\partial^2 v_z}{\partial z^2} \right) \quad (1c)$$

Where,

$\rho$  = fluid density

$g$  = gravity acceleration

$V_X, V_Y, V_Z$  = velocity in X, Y, Z direction

$t$  = time

$\eta$  = dynamic viscosity

$p$  = all around pressure.

The behavior of the fluid follows the partial differential equation which is based on conservation mass, Angular and Linear (Stokes law of equation), and Energy conservation.

Velocity in and around the spherical solid soil of radius 'a' is given as follows

$$v_r = v_o \cos \theta \left( 1 - \frac{3}{2} \frac{a}{r} + \frac{1}{2} \left( \frac{a}{r} \right)^3 \right) \quad (1d)$$

$$v_{\theta} = -v_{\infty} \sin \theta \left( 1 - \frac{3}{4} \frac{a}{r} + \frac{1}{4} \left\{ \frac{a}{r} \right\}^3 \right) \quad (1e)$$

$$v_{\phi} = 0 \quad (1f)$$

$$p = p_{\infty} - \frac{3}{2} \frac{\eta v_{\infty}}{a} \cos \theta \frac{a^2}{r^2} \quad (1g)$$

Where,

$v_{\infty}$  = free stream velocity

$a$  = ball radius

$r, \theta, \phi$  = coordinates of ball in 3D space.

$p_{\infty}$  = pressure at a distance 'r'

Continuity of scalar and mass balance equation is as follows

$$\frac{\partial p}{\partial t} + \frac{\partial \rho v_x}{\partial x} + \frac{\partial \rho v_y}{\partial y} + \frac{\partial \rho v_z}{\partial z} = 0 \quad (1h)$$

If  $\rho$  is constant

$$\frac{\partial \rho}{\partial t} = 0$$

Equation (1h) can be written as

$$\frac{\partial \rho v_x}{\partial x} + \frac{\partial \rho v_y}{\partial y} + \frac{\partial \rho v_z}{\partial z} = 0 \quad (1i)$$

Normal stress in spherical coordinates system is;

$$\sigma_{\eta} = 2\eta \frac{\partial v_r}{\partial r} \quad (1j)$$

Then according to Nerville stokes the shear stress will be

$$\tau_{r \theta} = \eta \left( \frac{1}{r} \frac{\partial v_r}{\partial \theta} + \frac{\partial v_{\theta}}{\partial r} - \frac{1}{r} v_{\theta} \right) \quad (1k)$$



## Chapter-3 Theory

### *3.1 Prediction methodologies*

The fundamental question that is related with landslide hazard assessment is “what will be the characteristic of slope failure?” Some landslides are slow or ductile, moving in a continuous or intermittent manner. Sometime it may cover long distances (earth flows), but the low velocity permits risk reduction action such as stabilization or evacuation to be taken. Others are brittle, it means that after a certain prelude of slow deformation, or due to sudden loading (e.g. during an earthquake), they accelerate and attains extremely rapid velocity maximum of 5 m/s or faster, it can exceed the speed of a running person. Such landslides are sometimes referred as “catastrophic”. But how can we recognize that whether the given potential landslides can become extremely rapid or not? The possible means of answering this question include judgmental approach; it is based on experience and comparison with precedents, experimental approach based on monitoring, and analytical approach based on limit equilibrium or stress-strain analysis.

### *3.2 Judgmental approach which is based on landslide typology*

From the experience, we know that some types of landslides behaves like a brittle manner, or it can be ductile in nature. But unfortunately, there is also a chance that they may exhibit brittle or ductile nature behaviour, or both. Nevertheless, a well-designed typological classification of landslides permits certain distinctions

to be made, at least on a preliminary basis. The following description of typical soil slide trends is based on Hungr et al. (2001).

Extra-sensitive (“quick”) clay flow slides are always extremely rapid events, both at initiation, and during flow-like travel. The same can be said about flow slides in loose saturated sands, often taking place under water. The term flow slide was given by Casagrande (1976) to signify a slide accompanied by liquefaction of a certain zone of saturated soil at the rupture point of surface, which invariably leads to catastrophic acceleration. Assumptions periodically appears in the literature that certain loose or dry fine grained soils can liquefy due to the air pressure in the pores. Most truly the dry granular flows are slow and it many extremely rapid flow slides appear to consist largely of dry or moist soil, with liquefaction affecting only a thin saturated layer at the base. These type of behaviour is observed in well-graded mine waste. Liquefaction of soil at the rupture point of surface may occur as a result of grain size crushing during the long-displacement sliding, as the modified grain size distribution of the crushed soil allows closer packing, accompanied by pore pressure increase. This could explain the spectacular mobility of many moderately deep-seated flow slides in residual soil, which probably begin by sliding on relict joints. Most shallow slides are occurring on steep slope which is extremely rapid, simply as a result of cohesion losses it starts the failure process (Hungr 2003). They are usually composed of loose granular surface overlying on stable substrate soil profile. Such types failures usually begin during the heavy rainfall, that confirm the suspended saturation of the loose soil layer. As soon the soil movement starts, soil situated on down-slope of the initial failure is over-ridden, by liquefying rapidly at un-drained loading and incorporated by growing the debris avalanche (Sassa 1985). When debris avalanches come into established steep stream

channels or gullies, they become channelized, combine further material as well as water and turn it into surging, extremely rapid debris flows.

### *3.3 Infinite slope theory*

The well known infinite slope model ( Haefeli, 1948; Taylor, 1948; Skempton and DeLory, 1957 ) can be used for analysing translational slope movement and as the geotechnical components and landscape evolution model that is basically combined together hydrological model to find out the pore water pressure and further find the probability of failure. The failed mass progresses along the planar surface that is parallel to the ground surface, with a just little rotary movement or the backward movement shows the characteristic of rotational slides failure. (Schuster and Krizek 1978). while the movement of the translational slide is controlled normally by the weak surfaces failure, such as joints, faults, or bedding planes, and the variations caused in shear strength between the different layers of deposited bedded. A cohesionless soil such as sandy banks, sand dunes or sandy banks, and levees. In the infinite slope for the analysis of homogeneous slopes, the slip surface can be assumed to be a plane which is parallel to the ground surfaces where its end effects is negligible and it can be neglected (Huang 1982).

The estimation of critical groundwater level for Landslide in Figure 3.1 below shows the the gravity forces and seepage erosion acting on an element from a slope of infinite slope. The governing equation is derived as follows and is given by Hong(2018).

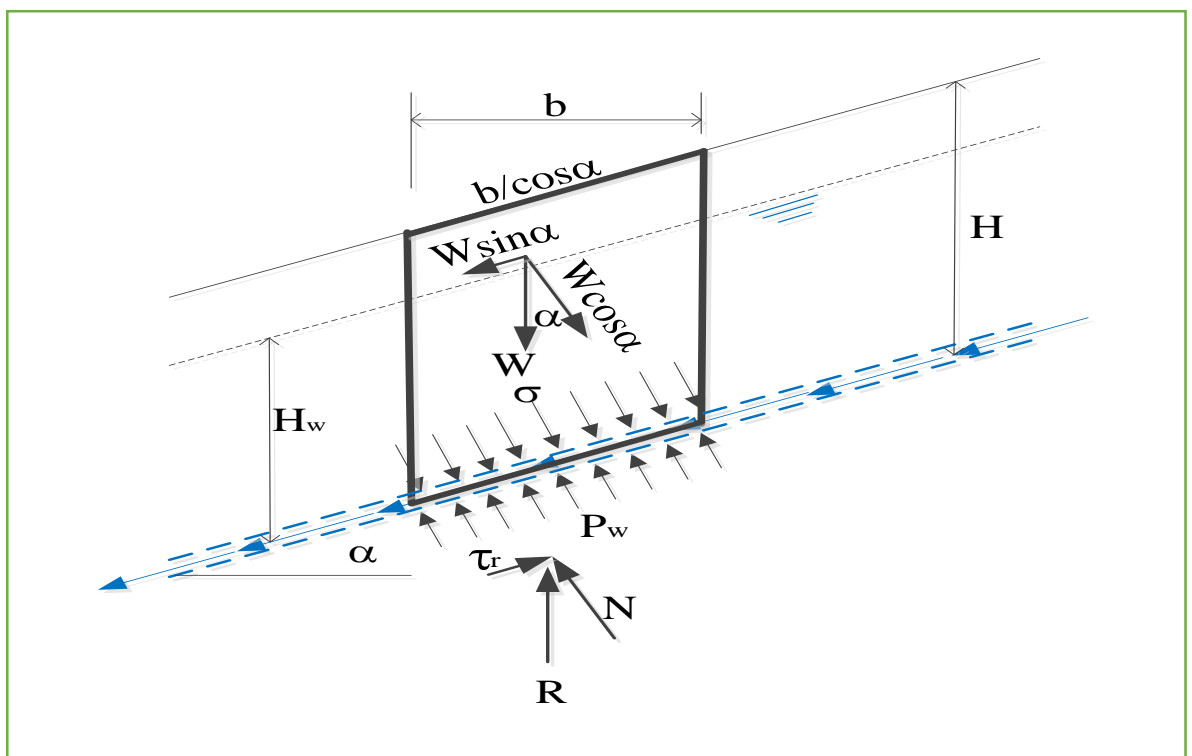


**Figure 3.1:** Forces acting and Seepage erosion occurring in the slip surface.



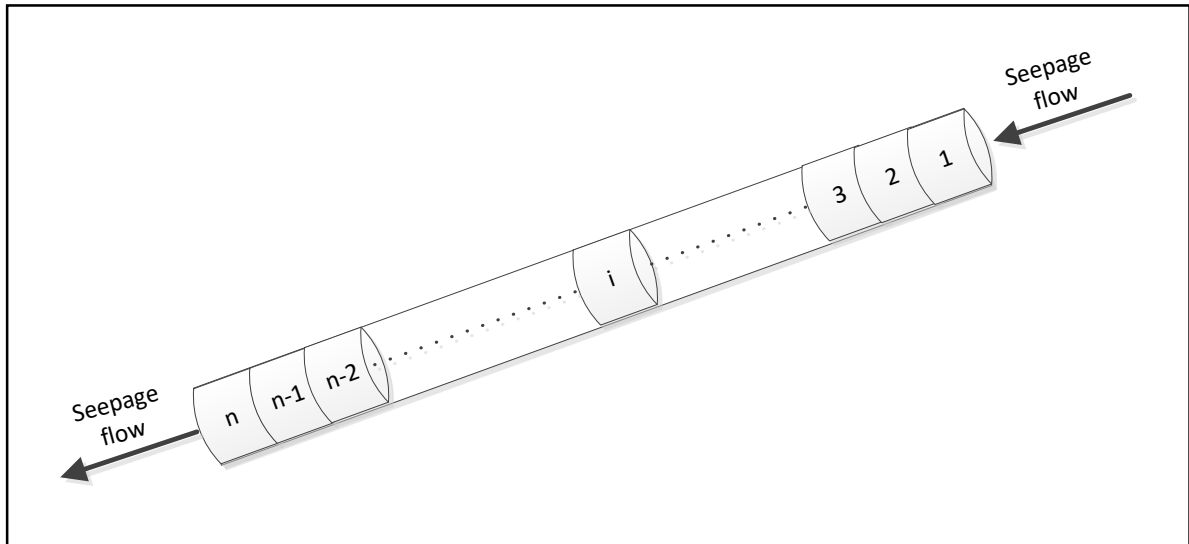


**Figure 3.2** Infinite slope

### 3.4 The infinite slope method

Infinite slope (IS) method is the simplest limit equilibrium method for slope stability analysis. Assuming the gravity of soil and water are the primary influences on changes for the movement of the slopes. The dynamics motion of the landslide are governed by the difference caused between the destabilize forces ( $\tau$ ), which basically depend on slope and weight, that are constant values, and the resisting forces ( $\tau_r$ ), which are very sensitive towards the water pressure at the slip slope surface.

By assuming, the forces in the perpendicular and parallel to the slope, the normal, lifting and shear stresses can be described as follows

$$\sigma = \frac{W \cos \alpha}{b / \cos \alpha} = \frac{\gamma b H \cos \alpha}{b / \cos \alpha} = \gamma H \cos^2 \alpha \quad (2a)$$

$$p_w = \frac{\gamma_w H_w \cos \alpha}{b / \cos \alpha} = \gamma_w H_w \cos^2 \alpha \quad (2b)$$

and

$$\tau = \frac{S}{b / \cos \alpha} = \frac{\gamma b H \sin \alpha}{b / \cos \alpha} = \gamma H \sin \alpha \cos \alpha \quad (2c)$$

Where  $\alpha$  is the slope angle;  $\gamma$  is the specific weight of solid;  $H$  is the height from slip slope to the surface;  $H_w$  is the height of slip slope to the height of water table. For the local points of the landslides where infinite slope conditions are applied, the resisting forces can be calculated by using Mohr-Coulomb failure criterion, that depending on friction and cohesion as follows:

$$\tau_r = c + (\sigma - p_w) \tan \varphi = c + (\gamma H - \gamma_w H_w) \cos^2 \alpha \tan \varphi \quad (2d)$$

Where  $\sigma$  is the normal stress,  $c$  is the cohesion,  $p_w$  is groundwater pressure, and  $\varphi$  is the internal friction angle, all magnitudes referred to the slip surface (Corominas et al. 2005).  $p_w$  is the temporal variable in the resisting shear stress. The critical condition occurs in  $\tau = \tau_r$ . A large GL will increase  $p_w$ , and decrease  $\tau_r$ , and induce landslide finally. Replacing Eq. (2), the threshold of groundwater level  $p_{wc}$  can be written as

$$P_{wc} = \sigma - (\tau - c) / \tan \varphi \quad (3a)$$

Substituting  $P_{wc}$  by  $H_{wc}$  by Equation (1b), the maximum groundwater level  $H_{wc}$  will be

$$H_{wc} = (\gamma/\gamma_w)H - (\gamma H \sin \alpha \cos \alpha - c)/(\gamma_w \cos^2 \alpha \tan \varphi) \quad (3b)$$

Equation (3b) displays that  $H_{wc}$  is the function of specific weight of solid and water, the resisting forces, the cohesion, the slope angle, and the friction angle.

### 3.5 Darcy law equation

Henry darcy law describes the flow of fluid through porous medium, this theory is based on the result of experiment. The equation below describes the laminar flow of fluid given by darcy.

$$q_o = \frac{K_o}{2\mu} A \left( \frac{\Delta p}{\Delta L} \right) \quad 4(a)$$

$q_o = \text{flow rate.}$

$\mu = \text{viscosity of fluid}$

$K_o = \text{permeability constant}$

$\frac{\Delta p}{\Delta L} = \text{hydrolic pressure gradient.}$

When seepage occur , the fine particles will be carried out by the seepage along the sliding surface as shown in the figure above .Khilar and fogler developed the pipe surge formula as given below.

$$\frac{\Delta P}{\Delta L} = \frac{\tau_c}{2.828} \left( \frac{n_o}{K_o} \right)^{1/2} \quad 4(b)$$

$\tau_c = \text{critical shear stress}$

$n_o = \text{porosity}$

The above Equation can be modified and written as

$$P_{wc} = \frac{\tau_c \Delta L}{2.828} \left( \frac{n_o}{K_o} \right)^{1/2} \quad 4(c)$$

By putting all the values of equation (4c) in the equation 3(b) and write it in the form of  $H_w$

$$H_{wc} = \frac{\tau_c}{2.828 r_w (\cos \alpha)^2} \left( \frac{n_o}{K_o} \right)^{1/2} \quad 4(d)$$

By equating the above equation with the equation 3(b) then we can get the equation for critical stream line as follows.

$$\Delta L = (\gamma H (\cos \alpha)^2 - (\gamma H \sin \alpha \cos \alpha - c) / (\tan \varphi)) \times \left( \frac{2.828}{\tau_c} \right) \times \left( \frac{K_o}{n_o} \right)^{1/2} \quad 4(e)$$

### 3.6 The Mohr coulomb failure criteria

In order to predict or know the potential for infinite slope to fail a very simple model is made to address the mechanical behaviour of the slope sediments under normal stress. Assume that the sediments behaves like Mohr coulomb material (Lambe and Whitman, 1969). This type of materials fails when the shear stress acting along the plane through the sediments exceeds its sediment shear that equation is given by the coulomb failure criterion (Jaeger and cook, 1979)

$$|\tau| = \sigma_n \tan \phi + S_o \quad 5(a)$$

Here

$\tau$  = the shear stress

$\sigma_n$  = the effective normal stress

$\phi$  = the friction angle of slope sediments

$S_o$  = Cohesion of sediments

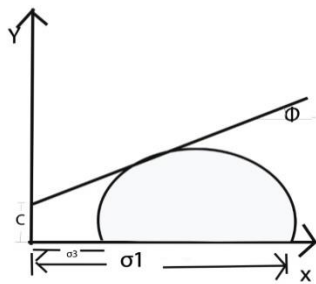


**Figure 3.3**

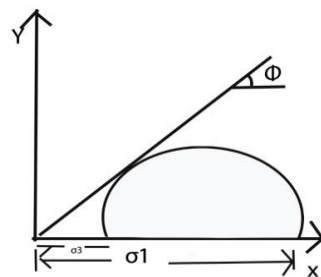


**Figure 3.4**

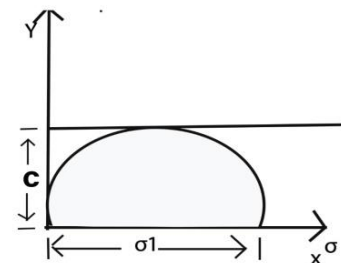


**Figure 3.5**

Cohesion less soil:- When the soil is purely granular then soil possess no cohesion ( $C=0$ ). And the shear strength of this type of soil is given by,

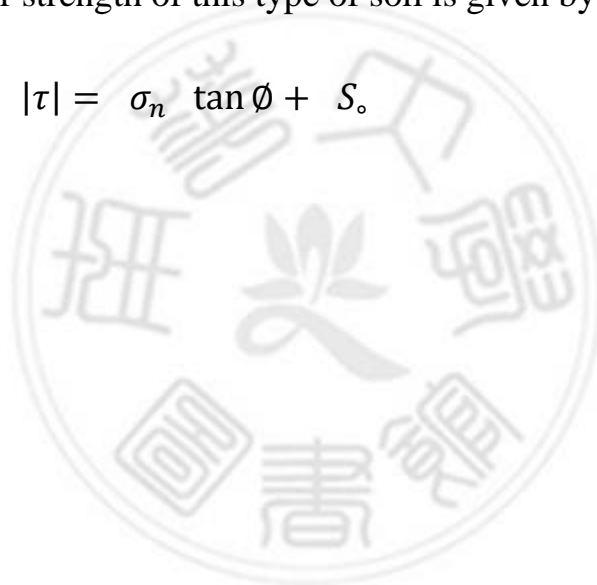
$$|\tau| = \sigma_n \tan \phi \quad 5(b)$$

Cohesive soil:- When the Fine soil possess cohesion but there is no friction between these fine particles ( $\phi = 0$ ) . The shear strength is given by,

$$|\tau| = S_0 \quad 5(c)$$

Cohesive frictional soil:- Soil which possess both cohesion and friction is called  $C\phi$  soil , The shear strength of this type of soil is given by

$$|\tau| = \sigma_n \tan \phi + S_0 \quad 5(d)$$



## Chapter-4 Outcome and discussion

### *4.1 Standard Proctor compaction test.*

The test consists of compacting the soil or the aggregate to be tested into a standard mould using a standardized compactive rammer at several different levels of moisture content. The maximum dry density and optimum moisture content is determined from the results of the test. Soil in place is tested for in-place dry bulk density, and the result is divided by the maximum dry density to obtain a relative compaction for the soil in place. In the other hand, soil compaction test is carried out in the laboratory in determining the ideal volume of water to be poured while compaction the soil on site so that the required compaction degree can be obtained. The moisture content recorded when the maximum dry unit weight is achieved is known as the optimum moisture content



**Figure 4.1:** Sand Sample

Governing Equation

$$\text{Density}(\rho) = \frac{\text{mass}}{\text{volume}}$$

$$\rho_d = \frac{\rho}{1+w} \quad (6a)$$

Calculation for dry density is displayed in table 3

**Table 3:** Calculation of dry density

water percentage	mass of mould + base plate (gm)	mass of mould + base plate + compacted soil (gm)	mass of compacted soil	Bulk density (g/cm <sup>3</sup> )	dry density(g/cm <sup>3</sup> )
4%	4085.5	5400.5	1315	1.39	1.336
6%	4085.5	5442	1356	1.43	1.356
8%	4085.5	5500	1415	1.5	1.39
10%	4085.5	5552	1466.5	1.55	1.419
12%	4085.5	5606	1520.5	1.61	1.444
14%	4085.5	5696	1583	1.67	1.462
16%	4085.5	5725	1639	1.73	1.481
18%	4085.5	5735	1649	1.74	1.486
20%	4085.5	5730	1644	1.74	1.458
22%	4085.5	5728	1642	1.74	1.424
24%	4085.5	5725	1639	1.73	1.402



**Table 4:** Calculation of water content

water percent age	mass of container + wet soil (gm)	mass of container + dry soil (gm)	mass of water (gm)	mass of container (gm)	mass of dry soil (gm)	water content %
4%	143	140	3.5	51.5	88	4
6%	118	114	3.5	53	61.5	5.7
8%	125	120	5	54.5	66	7.6
10%	121	115	5.5	55.5	60	9.2
12%	121	114	7	52	62	11.3
14%	253	245	8	190	55	14.5
16%	240	231	9	178	53	17
18%	337	328	9.5	273	55	17.3
20%	234	229	5.1	202	26.5	19.2
22%	92	85	7.5	50.5	34	22
24%	94	87	6.8	58	29	23.6

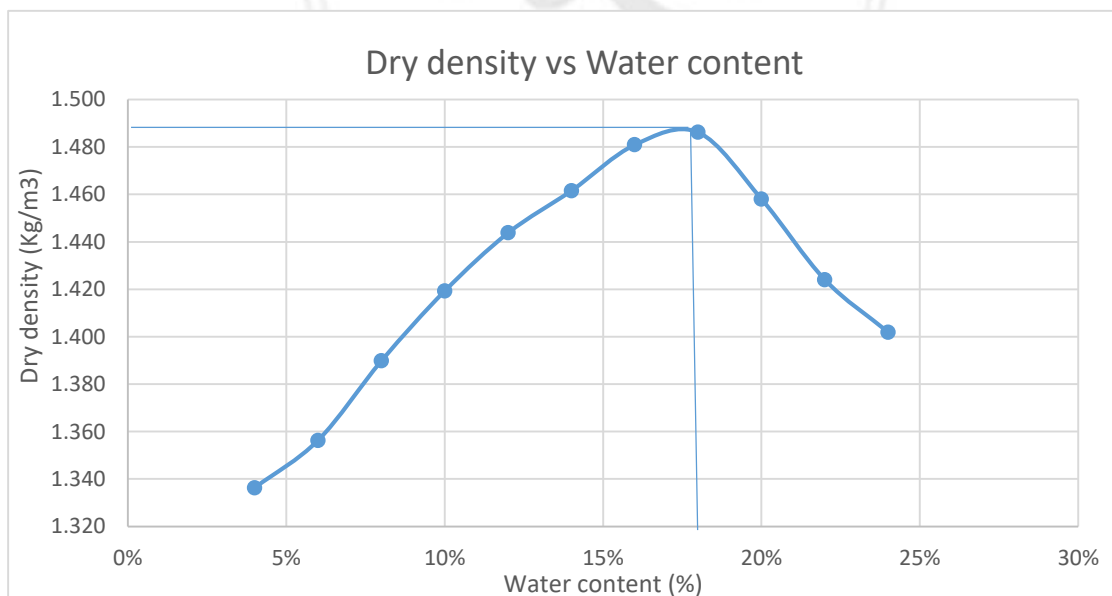


**Figure 4.2:** Optimal moisture content can be obtained by the relationship between water content and dry density

Hence from the peak point of the curve we get the corresponding value of Maximum dry density (MDD) and Water content are 1.482 g/cc and 17.8% respectively.

So we get OMC= 17.8% and MDD= 1.482 g/cc.

#### *4.2 Falling head permeability test*

The falling head permeability test involves flow of water through a relatively short soil sample connected to a standpipe which provides the water head and also allows measuring the volume of water passing through the sample. The diameter of the stand pipe basically depends on the permeability of the soil tested. The test can be carried out in a Falling Head permeability cell. Before starting the flow measurements, the soil sample is saturated and the standpipes are filled with de-aired water to a given level. The test then starts by allowing water to flow through the sample until the water in the standpipe reaches a given lower limit. The time required for the water in the standpipe to drop from the upper to the lower level is recorded. Often, the standpipe is refilled and the test is repeated for couple of times

The equation applicable for falling head permeability test

$$k = \frac{aL}{A \times \Delta t} \ln \frac{h_1}{h_2} \quad (6b)$$

Where

$A$  = Cross-sectional area of sample.

$a$  = Cross-sectional area of burette.

$h_1$  = Hydraulic head across the sample at initial phase ( $t = 0$ )

$h_2$  = Hydraulic head across the sample at final phase ( $t = t_{\text{test}}$ )



**Figure 4.3**



**Figure 4.4**

Figure 4.3 and 4.4 shows the permeability meter equipment, where area of cylinder 'a' ( $\text{cm}^2$ ) = 19.625  $\text{cm}^2$ , cross Sectional Area of Sample 'A' ( $\text{cm}^2$ ) = 80.873  $\text{cm}^2$ , and length of sample 'L' (cm) = 10 cm.

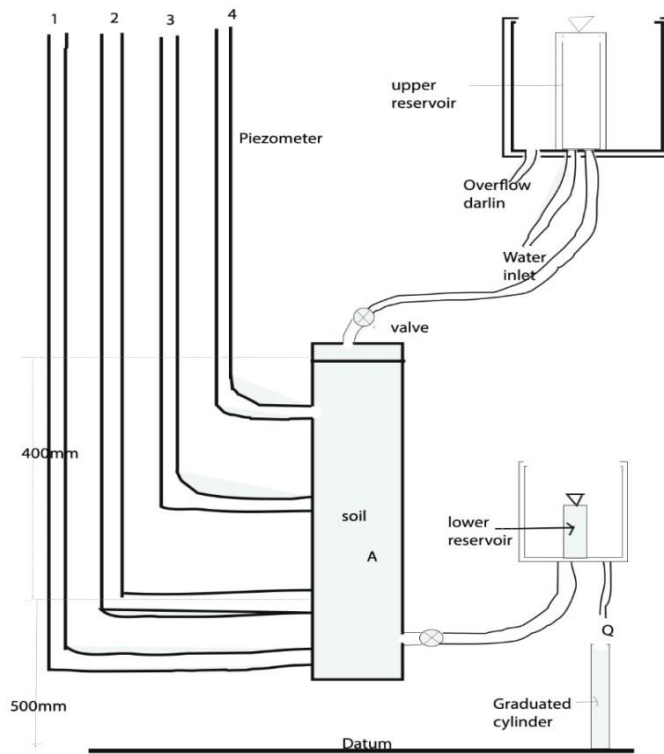


**Figure 4.5:** Configuration of permeability meter

**Table 5:** Permeability measurement

h1	h2	h1/h2	t (sec)
900	895	1.005586592	10
895	890	1.005617978	10
890	885	1.005649718	10
885	881	1.004540295	10
881	876	1.005707763	10
Average		1.005420469	

Average value of 'K' can be calculated by Equation (6b) and equals to  $1.35 \times 10^{-3}$  cm / sec.

### 4.3 Test for Threshold Pressure

No erosion filter test can be applied on the soil sample to find the optimum pressure at which water will pass through the sample. For the above experiment no filter was applied during the No erosion filter test. And the thickness of the sample was 14 cm. After the complete setup of soil sample in the cylindrical container, water with slow pressure start to enter in the cylinder. And then pressure start to increases continuously until water passes through the sample. The pressure at which water passes the soil sample that pressure is known as the threshold pressure. After the complete setup of soil sample in the cylindrical container, water with slow pressure start to enter in the cylinder. And then pressure start to increases continuously until water passes through the sample. The pressure at which water passes the soil sample that pressure is known as the threshold pressure



(a) Experimental setup for NEFT (b) Designed sample (c) Pressure

**Figure 4.6: No erosion filter test**

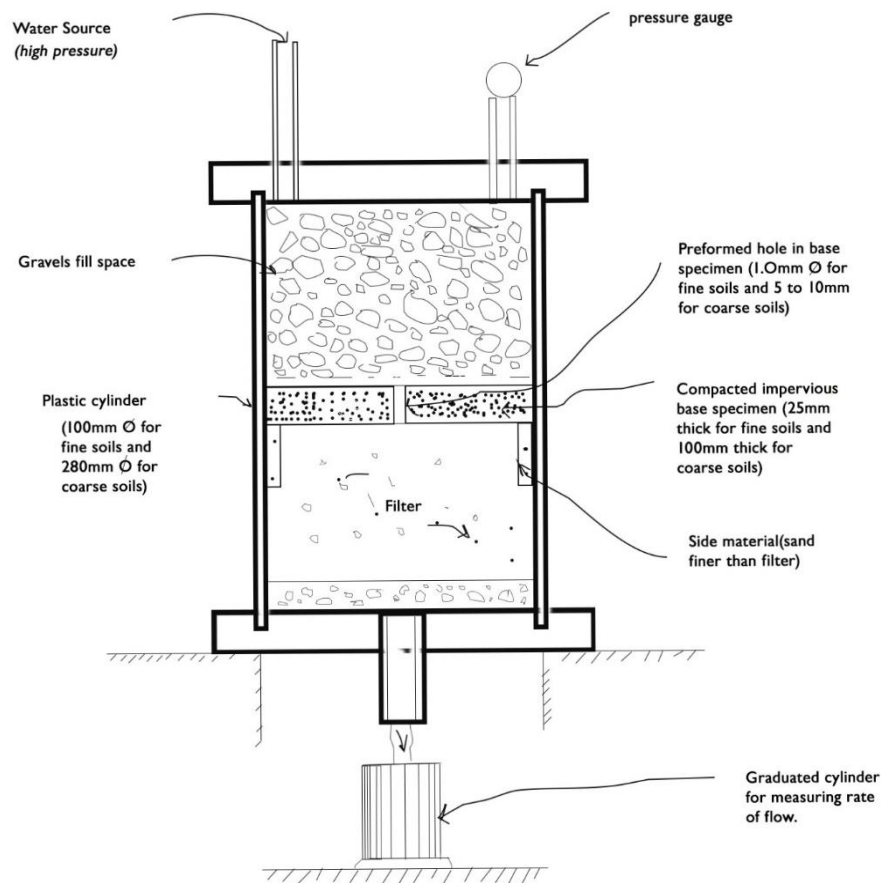


**Figure 4.7: Configuration of No erosion filter test**

From the experiment it was found to be the pressure of **2.45 Kg/cm<sup>2</sup>** as the threshold pressure.

#### 4.4 Tri-axial Test

A tri-axial shear test is a common method to measure the mechanical properties of many deformable solids, especially soil (e.g., sand, clay) and rock, and other granular materials or powders

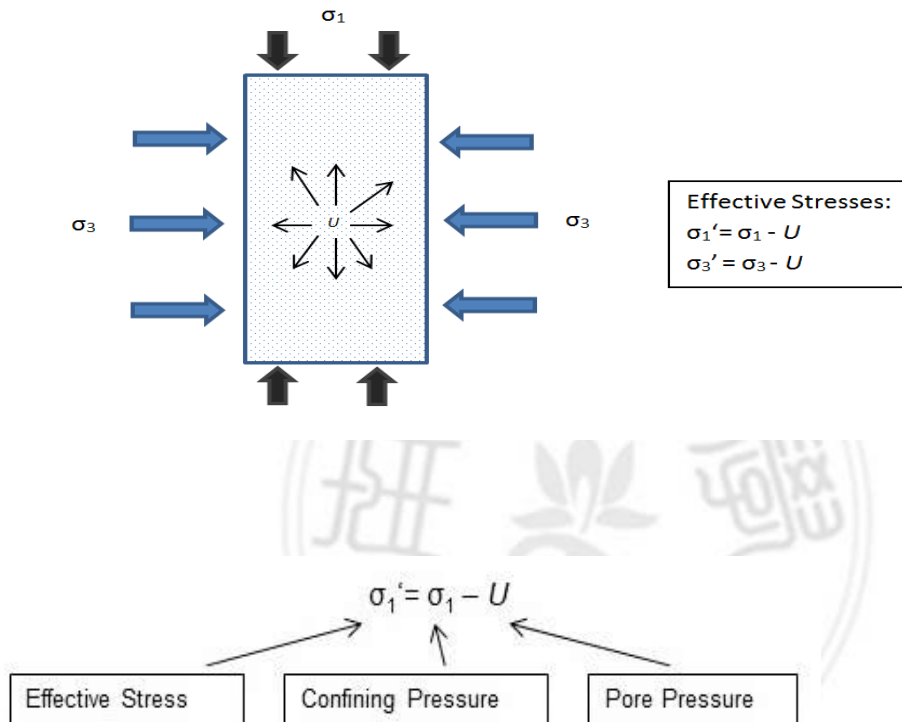


**Figure 4.8:** displays the physical meaning of tri axial shear test, where

$\sigma_1'$  – Effective Vertical (axial) Stress

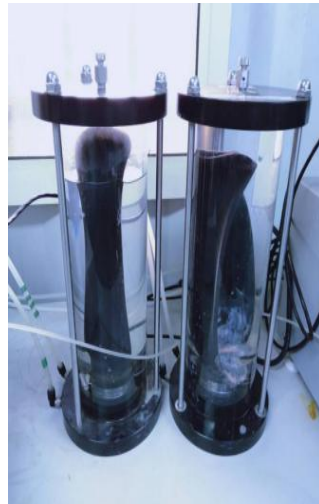
$\sigma_3'$  – Effective Confining Pressure

$U$  - Pore Pressure

$\sigma_1 - \sigma_3 =$  Deviator Stress (the stress due to the axial load applied to the specimen in excess of the confining pressure)



(a) Cell manual control



(b) Air/water control



(c) Tri axial cell



(a) Load frame



(e) Displacement transducer



(f) Volume controller

**Figure 4.9:** Equipment of Tri-axial Test



#### 4.4.1 Testing procedure:

The immersed permeable stone plate distance across same as the example is put on the platform of tri axial testing machine and the round channel paper of same size is put over the circle. Example is put on the channel paper. The channel paper with permeable stone is put on the example to permit two-way seepage.

- The latex film is extended in the layer cot and put on the dirt example. O rings are put at top and base of platens of the dirt example to forestall the phone water going into the example.
- The tri axial cell is put over the base and fixed with the screws. The cell is then loaded up with water and a little restricting weight of around 10 kPa is applied to hold the example set up.
- The dirt example should be totally soaked before isotropic union stage.
- Saturation process comprises of three stages: I) Water immersion, ii) Back weight application.
- Water immersion is finished by providing water from base of the example and permit it to leave the example from the top to do legitimate water flushing of the example. The water utilized for flushing should be refined and de-circulated water.

- The power immersion is performed by applying cell pressure and the back weight at consistent augmentations with steady contrast between these two weights. The example is permitted to soak for quite a while (10-20 min) after every augmentation of cell pressure and the back weight. This expansion ought to be trailed by a check for immersion esteem (B), otherwise called skempton's pore pressure boundary. Note that cell pressure consistently is higher than back weight. The example is supposed to be completely immersed if the B esteem more prominent than 0.95 can be procured. B is the proportion of pore pressure change because of the adjustment in cell stress ( $B = \Delta u / \Delta \sigma_{cell}$ ).
- Isotropic combination stage is begun by applying keeping pressure. During the Consolidation stage, seepage valve is kept open and the volume change is estimated until no adjustment in volume is watched (when essential solidification is finished).
- In the Consolidated Drained (CD) triaxial test, waste valves are kept open during shearing stage and volume change is estimated all through the test utilizing the volume change transducer.
- The stacking machine is gotten under way at a fitting strain rate dependent on the dirt kind (much lower strain rate than CU testing for same soil). Information obtaining framework (DAQ) is joined with the PC. load cell and transducers of triaxial framework, which records the information with the assistance of triaxial CD programming. The analysis is halted at around 15% strain.
- Three CD tests should be performed at three diverse picked binding weights



**Figure 4.10**

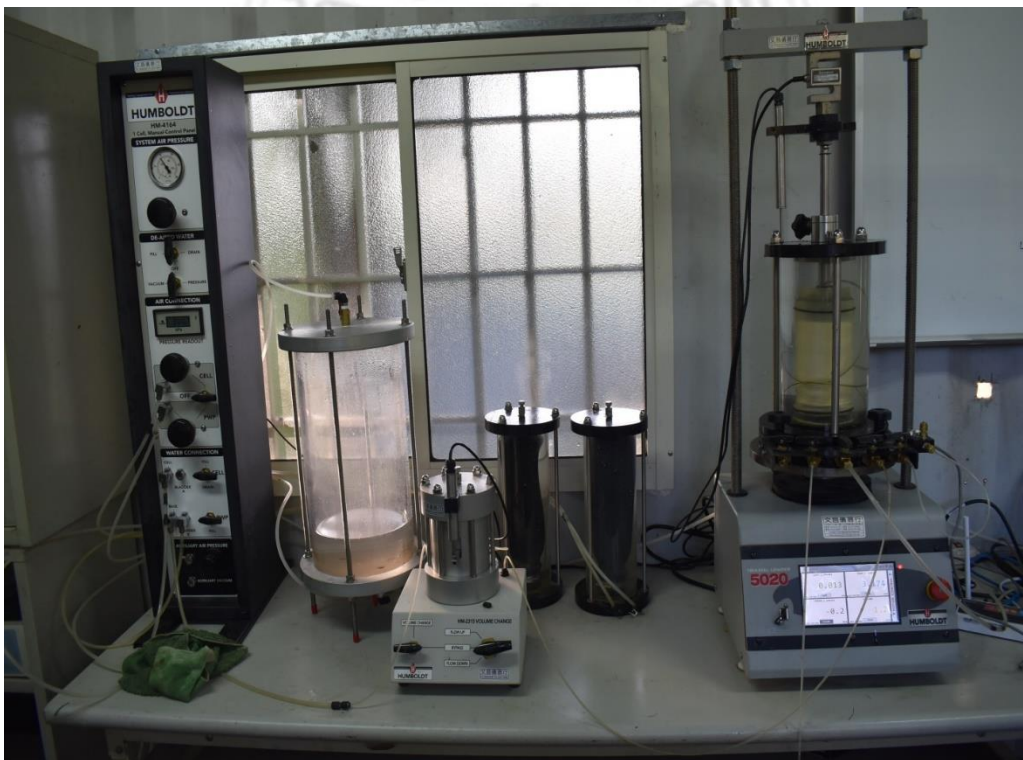


**Figure 4.11**

Figure 4.10 and Figure 4.11 display the experimental process.

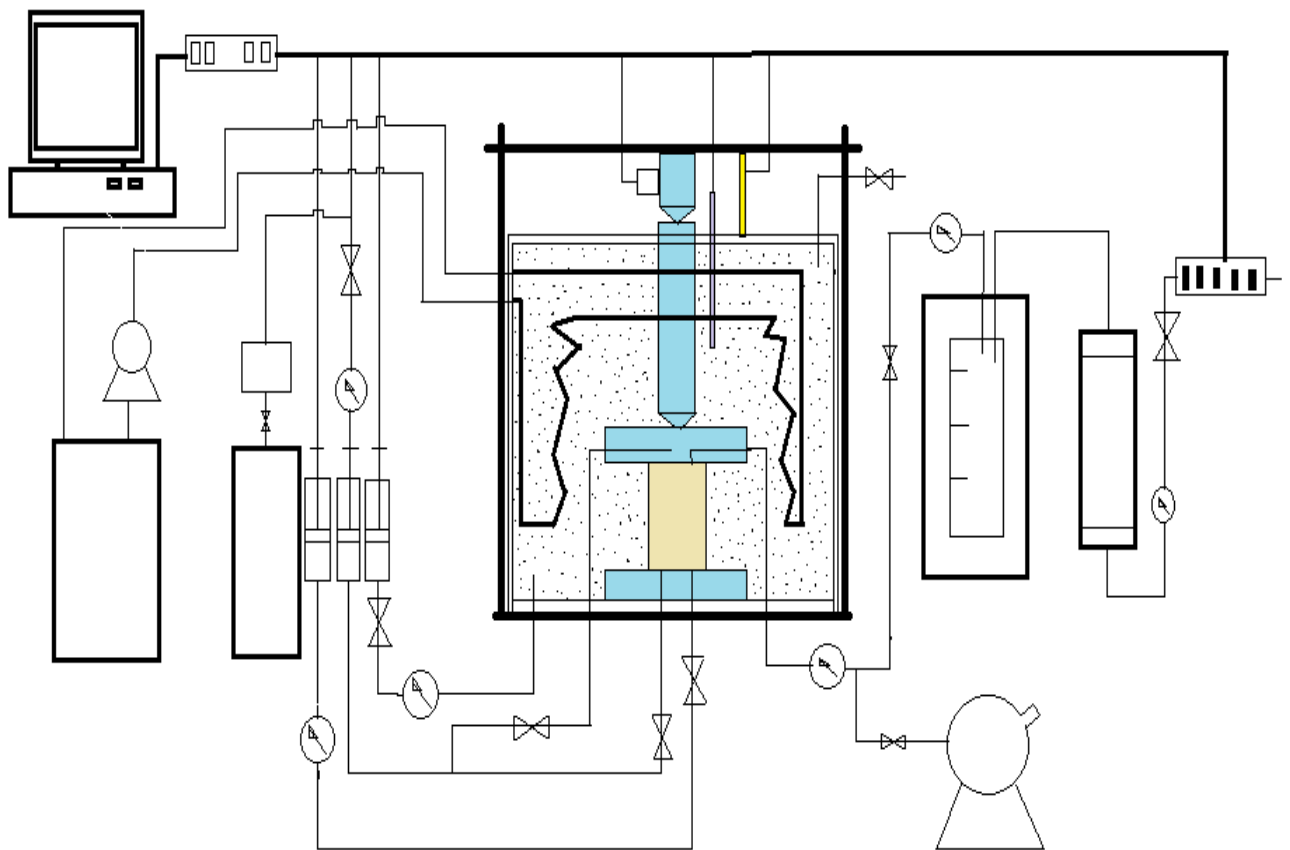


**Figure 4.12:** Schematic diagram of Tri-axial shear test experiment.

CD tests have been performed on sandy specimens at confining pressure of 10 kPa, 20 kPa, 30 kPa. All the tests were performed on normally consolidated soil specimens. The greater is the confining pressure, the greater the stress on the specimen, so that the specimen can be strained

The specimen was put under shear at strain rate of 0.005% per min after consolidation of specimen at chosen confining pressure. In all the tests, the saturation B value was obtained to be 0.97 before starting the consolidation phase of test, and the applied back pressure was put under control around 150 Kpa.

Graph between Deviator stress versus Axial strain curve were drawn along with the volumetric strain versus axial strain curves were plotted for all the three CU tri-axial tests.

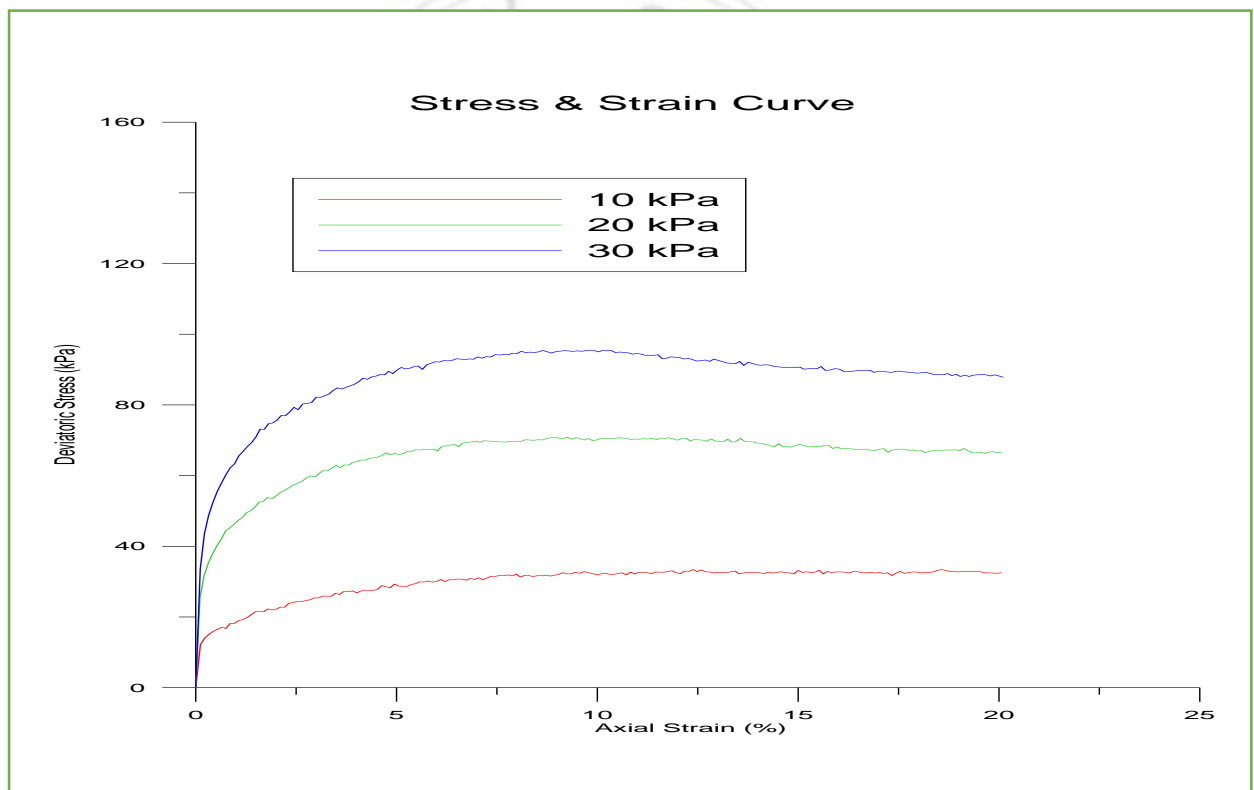


**Figure 4.13**

It can be seen from the stress strain curve figure 4.13 that at different confining pressure of 10kpa, 20kpa, and 30kpa, the property of stress and strain were

studied, it was found to be that stress is directly proportion to strain, so we can see it from graph that, greater the confining pressure the greater the stress on the specimen.

Effective stress analysis was performed on  $C_D$  tri axial tests as the pore pressure is zero because the drainage valve is kept open throughout the test. Total stress is the same as the effective stress during this test

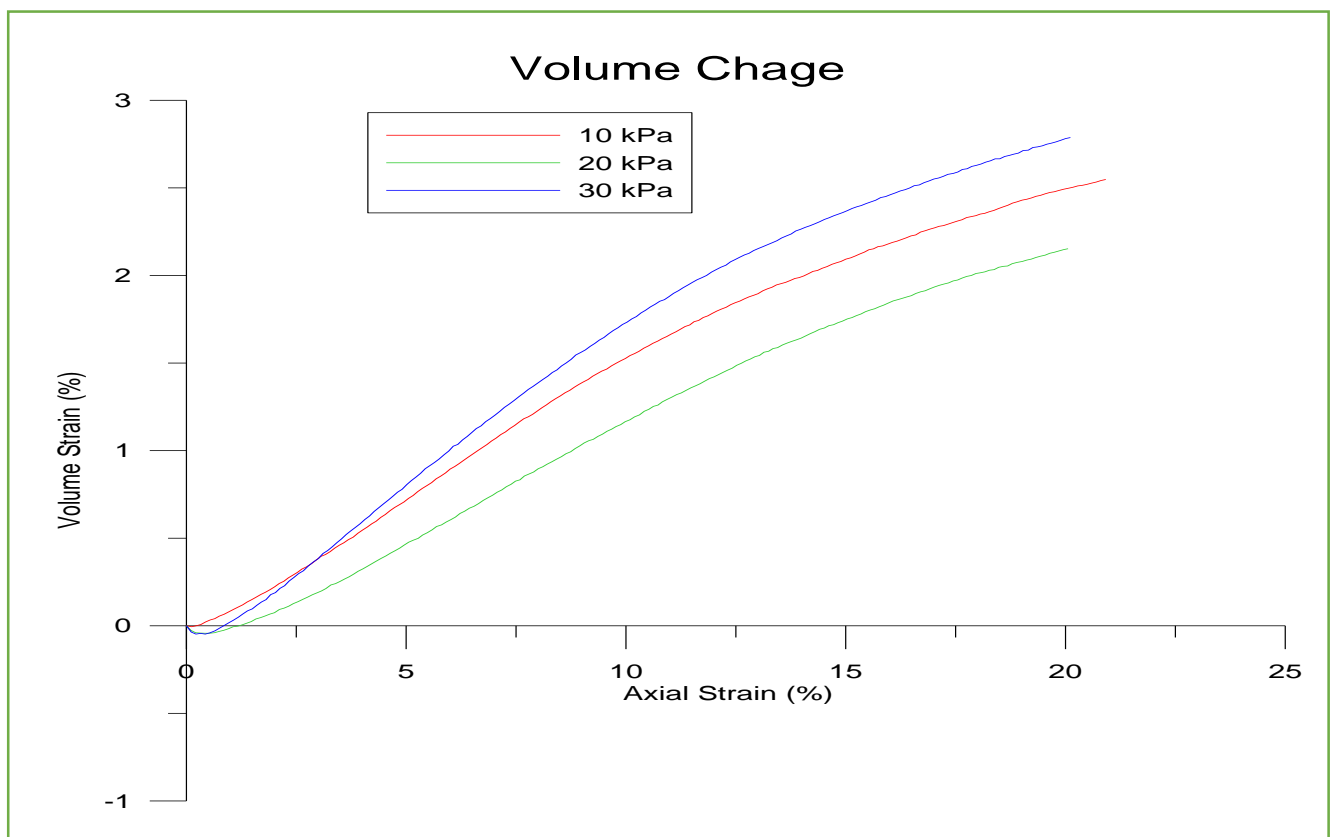


**Figure 4.14**

From the volume change Figure 4.14 it can be seen that at different confining pressure of ( 10kpa, 20kpa, 30kpa, ) three different and separate test were conducted on 3 different sample, it was found that if axial strain increases when

the confining pressure is 30kpa, then the volume change is greater than the volume change value for the 10kpa, 20kpa.

$$\text{Volumetric strain} = (\Delta V_s / V_c) \times 100$$

$\Delta V_s$  = volume change due to deviator stress during shearing stage phase.

$V_c$  = volume of specimen after the consolidation or before shearing stage

Volume of soil specimen after consolidation ( $V_c$ ) can be obtained by equation

$$V_c = V_0 - \Delta V_c$$

Where,

$\Delta V_c$  = volume change during consolidation

$V_0$  is the initial volume of the soil specimen

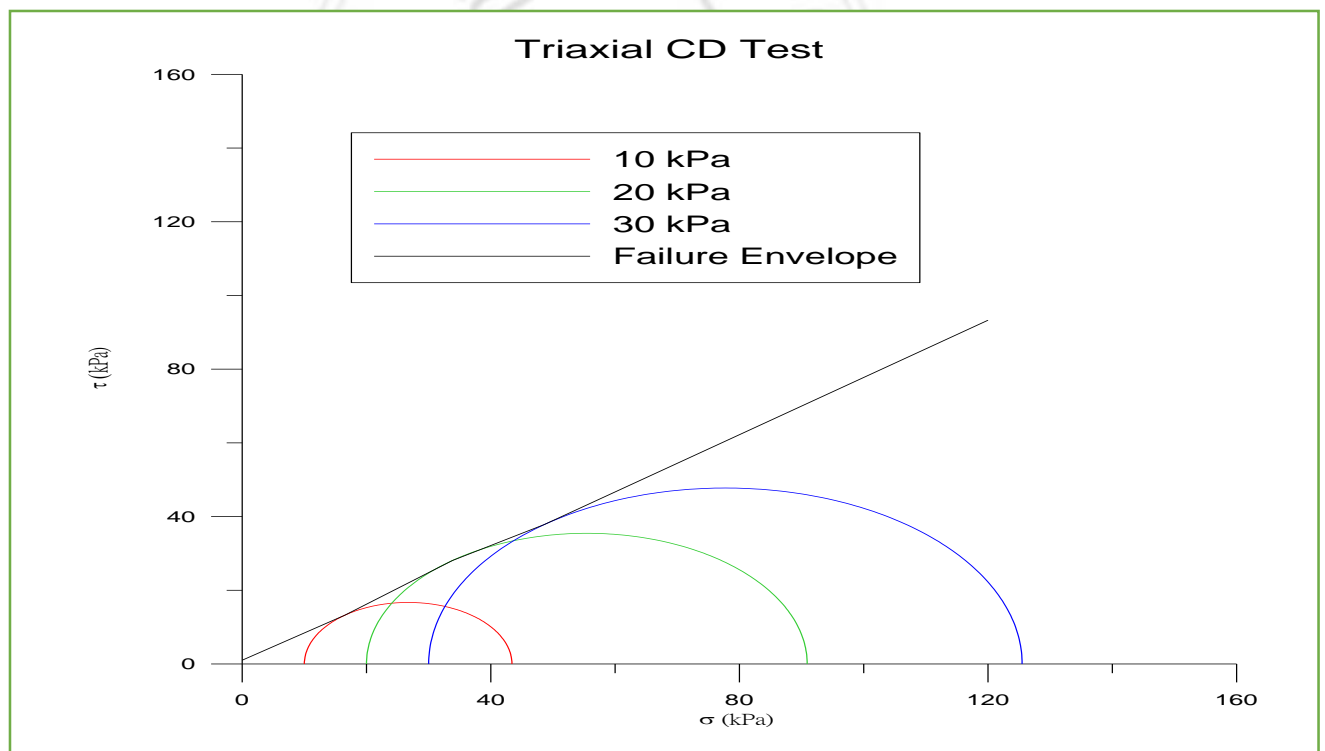


**Figure 4.15**

Mohr's circle is a geometrical representation of the state of stress in two dimensions. In one simple diagram, it represents the complete state of stress along any plane. One can interpret stress on different planes with different orientations. Mohr's circle for three dimensional state of stress consists of three separate circles touching one another with two circles completely inscribed within the outer larger circle.

Modified Failure envelop is obtained by drawing q-p curve for total stress analysis

$$q = (\sigma_1 - \sigma_3)/2, p = (\sigma_1 + \sigma_3)/2, \sigma_1 = \sigma_d + \sigma_3$$

Pore pressure is zero during shearing test in CD test, thus  $\sigma_3 = \sigma_3'$ ,  $\sigma_1 = \sigma_1'$ ,  $p = p'$

Finally Result obtained is given below,

$$\text{Cohesion} = 1.019 \text{ (newton /meter}^2\text{)}$$

Internal friction angle ( $\varphi$ )= 37 degree.

*Mathematical calculations,*

The best dry density obtained from laboratory experiment was 1.482 g/cc corresponding to 17.8 % maximum water content as shown previously. The soil sample used in the experiment is Quartz sand or white sand and its specific gravity taken as 2.67



$$\text{Density } (\gamma) = \frac{\text{Mass } (M)}{\text{Volume } (V)} = 1.482 \text{g/cc}$$

Calculating the void ratio by Assuming the total volume as 1.

$$V_t = 1 \quad ; \text{there for now,}$$

$$\text{Mass} = \text{density} \times \text{volume} = 1.482$$

$$\gamma_s = \frac{M}{V_s} = 2.67$$

$$V_s = \frac{M}{\gamma_s} = \frac{1.482}{2.67} = 0.55$$

$$\text{volume of voids} = (\text{total volume} - \text{volume of sand})$$

$$\text{volume of voids} = 1 - 0.55 = 0.45$$

$$\text{void ratio} = \frac{\text{volume of voids}}{\text{total volume}} = \frac{0.45}{1} = 45\%.$$

*Mathematical calculation and analysis based on the experiment,*

Experimental values as given as follows,

Maximum dry density = 1.482(g/cm<sup>3</sup>).

Optimal water content = 17.8%.

Water permeability = 1.35 × 10<sup>-3</sup> (cm/sec).

Cohesion = 1.019 (newton /meter<sup>2</sup>).

Internal friction angle (φ) = 37 degree.

Specific gravity = 2.67.

Void ratio = 0.45.

#### 4.4.2 Slope of critical ground water level

According to the theoretical formula 3(b) assume the different heights of as follows, H=20, 40, 60, 80, 100 meter. When the slope is equal to the internal friction angle  $\varphi=37$  degree then the water depth is 0, but still there will slippage.

$$H_{wc} = (\gamma/\gamma_w)H - (\gamma H \sin \alpha \cos \alpha - c)/(\gamma_w \cos^2 \alpha \tan \varphi) \quad (3b)$$

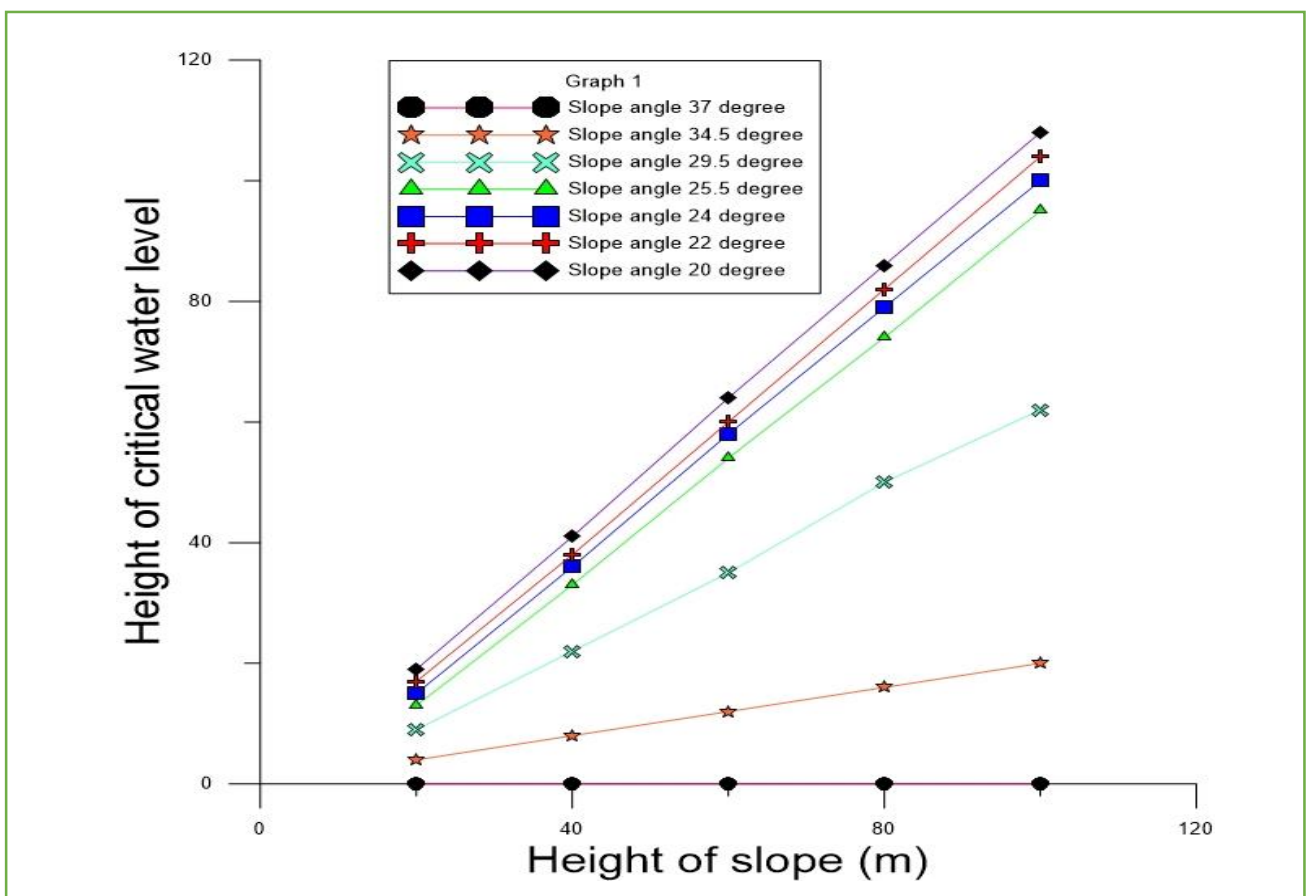


**Figure 4.16:** Slope of critical ground water level.

Boundary stream line length equation is given below

$$\Delta L = (\gamma H (\cos \alpha)^2 - (\gamma H \sin \alpha \cos \alpha - c) / (\tan \varphi)) \times \left( \frac{2.828}{\tau_c} \right) \times \left( \frac{K_o}{n_o} \right)^{1/2} \quad 5(a)$$

For a given height (h)=100 meter

$$\begin{aligned} \gamma &= 1 \quad H = 100 \text{ m} \quad C = 1.019 \text{ kpa} \quad \varphi = 37 \text{ degree} \\ K_o &= 1.35 \times 10^{-3} \quad n_o = 0.45 \end{aligned}$$

$$\tau_c = \frac{S}{b / \cos \alpha} = \frac{\gamma b H \sin \alpha}{b / \cos \alpha} = \gamma H \sin \alpha \cos \alpha$$

$$\tau_c = 1 \times 100 \times \sin(37) \cos(37)$$

$$\tau_c = 48.06$$

There for critical stream line length is as follows.

$$\begin{aligned} \Delta L &= (1 \times 100 (\cos 37)^2 - (1 \times 100 \sin(37) \cos(37) \\ &\quad - 1.019) / (\tan(37)) \times \frac{2.828}{48.06} \times \left( \frac{1.35 \times 10^{-3}}{0.45} \right)^{1/2} \end{aligned}$$

$$\Delta L = 58.1 \text{ m}$$

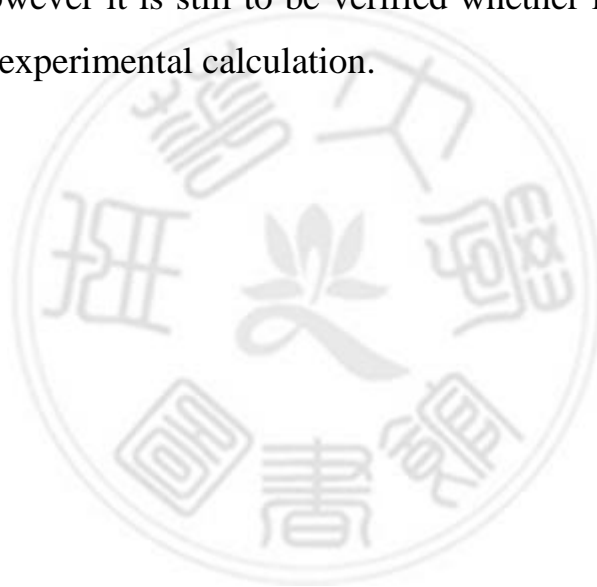
## Chapter-5 Discussion

After obtaining the real time rainfall and groundwater level data for the next unit of hour is predicted. This study only draws data from the experiment the values of critical groundwater level and critical streamline length of the infinite slope theory are used to estimate the slope failure. However different site will have different experimental values and it is not constant everywhere. In this study the Tri-axial test, proctor compaction test, falling head permeability test, related to school of civil engineering research test is done to know the properties and profile of soil. This test mainly verify the Hong (2018) established theory of infinite slope theory and a deep collapse theory failure of seepage flow. And through the test, we calculate the theoretical parameters of collapse failure and gradually pass the tri-axial test to calculate the parameter of infinite slope also at the same time use the permeability coefficient of test of Darcy's law to calculate the permeability coefficient ,and design a hypothetical slope to explain the parameters brought into the equation of failure theory to estimate the underground position of collapse ,length of seepage flow and the critical fracture position of slope, the calculated data can be used to design and manufacture of infinite slope.

## Chapter-6 Conclusions

In this study, the tri-axial test, compaction test and variable head penetration test were done to obtain the equation parameters for estimation of critical groundwater level of slope failure theory, and these critical groundwater level values may cause slope failure or trigger landslide

The data extracted from the experiment for the calculation of critical groundwater level and critical streamline length of infinite slope theory is used to estimate the slope failure but however it is still to be verified whether it will be used in the actual site after the experimental calculation.



## References

1. Al-Khafaji, A. W. N., & Andersland, O. B. (1992). Equations for compression index approximation. *Journal of geotechnical engineering*, 118(1), 148-153.
2. Baum, R. L., Godt, J. W., & Savage, W. Z. (2010). Estimating the timing and location of shallow rainfall-induced landslides using a model for transient, unsaturated infiltration. *Journal of Geophysical Research: Earth Surface*, 115(F3).
3. Bennethum, L. S., Murad, M. A., & Cushman, J. H. (1997). Modified Darcy's law, Terzaghi's effective stress principle and Fick's law for swelling clay soils. *Computers and Geotechnics*, 20(3-4), 245-266.
4. Boyd, R. H. (1961). Extension of Stokes' law for ionic motion to include the effect of dielectric relaxation. *The Journal of Chemical Physics*, 35(4), 1281-1283.
5. Budhu, M., & Gobin, R. (1996). Slope instability from ground-water seepage. *Journal of hydraulic Engineering*, 122(7), 415-417
6. Corominas, J., Moya, J., Ledesma, A., Lloret, A., & Gili, J. A. (2005). Prediction of ground displacements and velocities from groundwater level changes at the Vallcebre landslide (Eastern Pyrenees, Spain). *Landslides*, 2(2), 83-96.
7. Crosta, G., & Prisco, C. D. (1999). On slope instability induced by seepage erosion. *Canadian Geotechnical Journal*, 36(6), 1056-1073.

8. Cruden, D. M., & Varnes, D. J. (1996). Landslides: investigation and mitigation. Chapter 3-Landslide types and processes. *Transportation research board special report*, (247).
9. Dunne, T. (1990). Hydrology, mechanics, and geomorphic implications of erosion by subsurface flow. In *Groundwater Geomorphology: The Role of Subsurface Water in Earth-Surface Processes and Landforms* (Vol. 252, pp. 1-28).
10. Furuya, G., Sassa, K., Hiura, H., & Fukuoka, H. (1999). Mechanism of creep movement caused by landslide activity and underground erosion in crystalline schist, Shikoku Island, southwestern Japan. *Engineering geology*, 53(3-4), 311-325.
11. Gardner, W. R. (1958). Some steady-state solutions of the unsaturated moisture flow equation with application to evaporation from a water table. *Soil science*, 85(4), 228-232.
12. Ghiassian, H., & Ghareh, S. (2008). Stability of sandy slopes under seepage conditions. *Landslides*, 5(4), 397-406
13. Godt, J. W., Şener-Kaya, B., Lu, N., & Baum, R. L. (2012). Stability of infinite slopes under transient partially saturated seepage conditions. *Water Resources Research*, 48(5).
14. Griffiths, D. V., Huang, J., & Fenton, G. A. (2011). Probabilistic infinite slope analysis. *Computers and Geotechnics*, 38(4), 577-584.
15. Horton, R. E. (1936). Maximum ground-water levels. *Eos, Transactions American Geophysical Union*, 17(2), 344-357.

16. Hungr, O., Corominas, J., & Eberhardt, E. (2005). Estimating landslide motion mechanism, travel distance and velocity. In *Landslide risk management* (pp. 109-138). CRC Press
17. Hungr, O., Leroueil, S., & Picarelli, L. (2014). The Varnes classification of landslide types, an update. *Landslides*, 11(2), 167-194.
18. Hutchinson, J. W. (1968). Plastic stress and strain fields at a crack tip. *Journal of the Mechanics and Physics of Solids*, 16(5), 337-342.
19. Iverson, R. M., & Major, J. J. (1986). Groundwater seepage vectors and the potential for hillslope failure and debris flow mobilization. *Water Resources Research*, 22(11), 1543-1548
20. Ji, L., Zhang, T., Milliken, K. L., Qu, J., & Zhang, X. (2012). Experimental investigation of main controls to methane adsorption in clay-rich rocks. *Applied Geochemistry*, 27(12), 2533-2545
21. Khilar, K. C., & Fogler, H. S. (1998). *Migrations of fines in porous media* (Vol. 12). Springer Science & Business Media.
22. Koolen, A. J., & Vaandrager, P. (1984). Relationships between soil mechanical properties. *Journal of Agricultural Engineering Research*, 29(4), 313-319.
23. Lu, N., & Godt, J. (2008). Infinite slope stability under steady unsaturated seepage conditions. *Water Resources Research*, 44(11).



24. Milledge, D. G., Griffiths, D. V., Lane, S. N., & Warburton, J. (2012). Limits on the validity of infinite length assumptions for modelling shallow landslides. *Earth Surface Processes and Landforms*, 37(11), 1158-1166.
25. Muntohar, A. S., & Liao, H. J. (2009). Analysis of rainfall-induced infinite slope failure during typhoon using a hydrological–geotechnical model. *Environmental geology*, 56(6), 1145-1159
26. Muntohar, A. S., & Liao, H. J. (2010). Rainfall infiltration: infinite slope model for landslides triggering by rainstorm. *Natural hazards*, 54(3), 967-984.
27. Reddi, L. N., & Bonala, M. V. (1997). Critical shear stress and its relationship with cohesion for sand. kaolinite mixtures. *Canadian geotechnical journal*, 34(1), 26-33.
28. Richards, L. A. (1931). Capillary conduction of liquids through porous mediums. *Physics*, 1(5), 318-333
29. Salmasi, F., Pradhan, B. & Nourani, B. Prediction of the sliding type and critical factor of safety in homogeneous finite slopes. *Appl Water Sci* 9, 158 (2019)
30. Schuster, R. L., & Krizek, R. (1978). Landslides: analysis and control. *Unknown*.
31. Skempton, A. W. (1970). First-time slides in over-consolidated clays. *Geotechnique*, 20(3), 320-324.

32. Taylor, D. W. (1948). *Fundamentals of soil mechanics* (Vol. 66, No. 2, p. 161). LWW
33. Tek, M. R. (1957). Development of a generalized Darcy equation. *Journal of Petroleum Technology*, 9(06), 45-47.
34. Travis, Q. B., Houston, S. L., Marinho, F. A., & Schmeeckle, M. (2010). Unsaturated infinite slope stability considering surface flux conditions. *Journal of geotechnical and geoenvironmental engineering*, 136(7), 963-974.
35. Tsai, T. L., & Chiang, S. J. (2013). Modeling of layered infinite slope failure triggered by rainfall. *Environmental earth sciences*, 68(5), 1429-1434.
36. Vanacker, V., Vanderschaeghe, M., Govers, G., Willems, E., Poesen, J., Deckers, J., & De Bievre, B. (2003). Linking hydrological, infinite slope stability and land-use change models through GIS for assessing the impact of deforestation on slope stability in high Andean watersheds. *Geomorphology*, 52(3-4), 299-315
37. Yu, M. H., & He, L. N. (1992). A new model and theory on yield and failure of materials under the complex stress state. In *Mechanical Behaviour of Materials VI* (pp. 841-846). Pergamon